Adsorption (2014) 20:769–776
DOI 10.1007/s10450-014-9620-1

Evaluating methane storage targets: from powder samples to onboard storage systems

B. P. Prajwal · K. G. Ayappa

Received: 8 November 2013 / Revised: 12 May 2014 / Accepted: 17 June 2014 / Published online: 29 June 2014

Abstract The development of a viable adsorbed natural gas onboard fuel system involves synthesizing materials that meet specific storage target requirements. We assess the impact on natural gas storage due to intermediate processes involved in taking a laboratory powder sample to an onboard packed or adsorbent bed module. We illustrate that reporting the V/V (volume of gas/volume of container) capacities based on powder adsorption data without accounting for losses due to pelletization and bed porosity, grossly overestimates the working storage capacity for a given material. Using data typically found for adsorbent materials that are carbon and MOF based materials, we show that in order to meet the Department of Energy targets of 180 V/V (equivalent STP) loading at 3.5 MPa and 298 K at the onboard packed bed level, the volumetric capacity of the pelletized sample should be at least 245 V/V and the corresponding gravimetric loading varies from 0.175 to 0.38 kg/kg for pellet densities ranging from 461.5 to 1,000 kg m^{-3}. With recent revision of the DOE target to 263 V/V at the onboard packed bed level, the volumetric loadings for the pelletized sample should be about 373 V/V.

Keywords Gravimetric capacity · Powder · Pellet · Adsorbed natural gas · Storage target

B. P. Prajwal · K. G. Ayappa (✉)
Department of Chemical Engineering, Indian Institute of Science, Bangalore, India
e-mail: ayappa@chemeng.iisc.ernet.in

1 Introduction

Among alternate transportation fuels, natural gas has emerged as a lower emission fuel substitute for gasoline. Compressed natural gas (CNG) is used in many countries for public transportation. However safety considerations due to the high pressures (20–25 MPa) involved are a limiting factor. To overcome pressurization costs and safety issues, technologies based on adsorbed natural gas (ANG) are being actively pursued. Several challenges are associated with developing a commercially robust and economically viable onboard ANG storage system. The starting point is the search for materials that meet storage targets set by the Department of Energy (DOE). The 180 $(V/V)_b$ storage target at STP conditions (Burchell and Rogers 2000) requires that the volume of methane stored in an adsorbent or packed bed of volume V_b is $180V_b$ at STP conditions. The DOE has recently revised the methane storage targets for packed adsorbents to have gravimetric capacity more than 0.5 kg/kg (Advanced Research Project Agency, U.S DOE 2012) and volumetric capacity of 263 $(V/V)_b$ at the adsorbent or packed bed stage which is equivalent to the volumetric storage capacity of CNG at 250 bar and 298 K (Mason et al. 2014). We use the subscript 'b', 'p', and 'pwd' to differentiate the V/V capacities for bed, pellet and powder respectively.

2 Achieving targets

Synthesized powder samples are tested for their adsorption capacity using either gravimetric or volumetric methods. In order for a material to be used on an onboard device the material is pelletized or extruded (0.5–1 mm) to reduce the pressure drop in the adsorbent bed. The process of

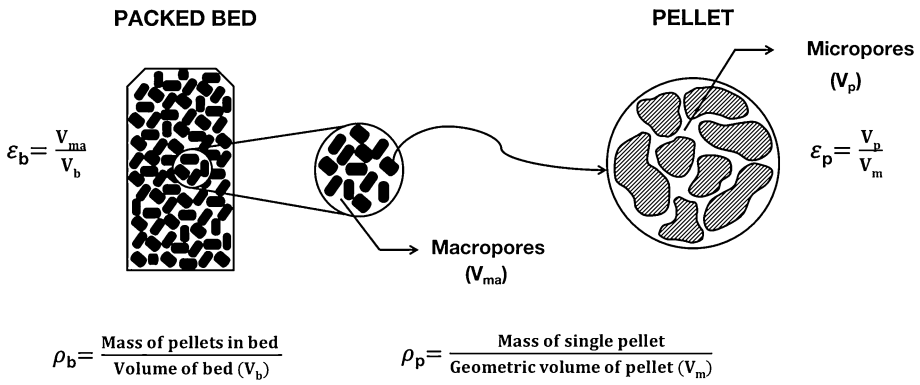

Fig. 1 Schematic illustrating the macropores in the packed bed, micropores in the pellet and their relationship to the bed porosity (ϵ_b) and pellet porosity (ϵ_p) respectively. Equations 2–4 relate the porosities to the respective densities ρ_b and ρ_p. Micropore volume in pellet, V_p; macropore volume in packed bed, V_{ma}; volume of the bed, V_b; geometric volume of the pellet, V_m

pelletization involves compaction with or without a binder, invariably results in a loss of surface area and/or pore volume. Consequently, the adsorption capacity of the pellet is lower than that of the powder sample. The resulting drop in gravimetric capacity typically ranges between 5 and 20 % (Celzard et al. 2005; Inomata et al. 2002; Tagliabue et al. 2011; Lozano-Castelló et al. 2002). When pellets are packed into an adsorbent bed, there is a further decrease in the capacity due to the inherent porosity (void space) in the adsorbent bed (Fig. 1). The total porosity is typically in the range of 0.6–0.7 (Mota et al. 1997; Sahoo et al. 2011, 2014b; Bastos-Neto et al. 2005). The final decrease in capacity is encountered at the time of onboard filling of the adsorbent bed. Gas filling is highly exothermic with adsorbent bed temperatures typically rising by about 50–80 K (Sahoo et al. 2011, 2014a; Mota et al. 1997; Basumatary et al. 2005; Goetz and Biloé 2005; Biloé et al. 2002). As a result filling efficiencies range between 70 and 80 % (Biloé et al. 2002; Goetz and Biloé 2005; Sahoo et al. 2011, 2014a). This last drop in capacity can be circumvented with a slow off-board fill under nearly isothermal conditions. Given this sequence, a material must meet the storage target accounting for losses in adsorption capacity incurred while taking the material from the powder form to the adsorbent bed module used in an onboard device.

Hence assessing laboratory prepared powder samples under isothermal conditions, grossly overestimates the adsorption capacity (vis-à-vis DOE targets) for a material. This overestimate is further magnified if the skeletal or single crystal density is used (Mason et al. 2014; Sun et al. 2009; Konstas et al. 2012). However, this is perhaps the most widespread measure by which materials are currently assessed in the literature (Peng et al. 2013; Makal et al. 2012).

Exceptions occur in carbon monoliths which are high density carbon structures with reduced porosity. In this specific case, losses associated with pelletization and packed bed porosity are circumvented (Matranga et al. 1992). We show that in order to achieve the DOE target of 180 $(V/V)_b$ in the adsorbent bed, the adsorption capacity of the pellets must be at least 36 % (245 $(V/V)_p$) greater to

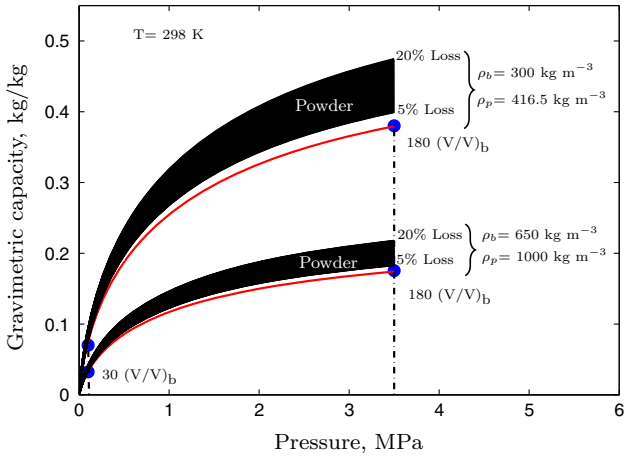

Fig. 2 Excess gravimetric adsorption isotherm for pellet and powder sample meeting the 180 $(V/V)_b$ at 3.5 MPa and 298 K illustrated for different values of bed density, ρ_b. For a given pellet density, the bands illustrate the increase in gravimetric capacity at the powder level in order to meet the 180 $(V/V)_b$ storage targets. We consider a gravimetric capacity loss ranging for 5–20 % during pelletization. The *red lines* are fits to the Dubinin-Ashtakov model. *Blue filled circles* indicate the bed storage capacity, $(V/V)_b$ at 3.5 and 0.1 MPa. ρ_p values are obtained from Eq. 4 with $\epsilon_b = 0.35$ (Color figure online)

account for pelletization and packed bed losses. We also evaluate the gravimetric loading (weight of methane gas/weight of adsorbent) capacity for both the pellet and powder samples at various volumetric storage targets. In order to meet storage targets, materials should be evaluated in the pelletized form after taking into account the adsorption losses during the powder to pelletization process. To quantify this situation we use typical physical properties reported for activated carbons and MOF adsorbents.

2.1 Packed bed model

Let us consider an onboard ANG adsorbent bed of volume V_b made up of pellets. The total mass of gas stored in the bed is,

$$m_g = V_b \rho_g \epsilon_t + V_b \rho_b q_p, \quad (1)$$

where the first term on the right hand side represents the mass of methane present in the gaseous phase and the second term is the amount of adsorbed gas in the pellet. In the above equation, ρ_g is the methane gas density, ϵ_t is the total bed porosity, ρ_b is the bed density and q_p is the gravimetric adsorption capacity of the pellet.

The relationships between the various porosities and densities used routinely in packed bed studies are given below (Kumar et al. 2009). Figure 1 is a schematic illustrating the different porosities encountered in packed beds.

$$\rho_b = \rho_s(1 - \epsilon_t), \quad (2)$$

where ρ_s is the skeletal or single crystal density and ϵ_t is the total bed porosity. The pellet density,

$$\rho_p = \rho_s(1 - \epsilon_p), \quad (3)$$

where ϵ_p is the pellet porosity. Combining Eqs. 2 and 3 with the relation, $\epsilon_t = \epsilon_b + (1 - \epsilon_b)\epsilon_p$ we get,

$$\rho_b = (1 - \epsilon_b)\rho_p. \quad (4)$$

The equivalent mass of methane gas, m_g corresponding to a 180 $(V/V)_b$ (STP) storage capacity for a bed of volume V_b is,

$$m_g = \frac{180 V_b M_g}{22.414}\ (\text{kg}), \quad (5)$$

where V_b is the volume of the adsorbent bed in m^3 and $M_g = 16.03$ is the molecular weight of methane. For a given value of m_g, the corresponding value of q_p can be obtained from Eq. 1 after having specified ρ_b and ϵ_t. We fix $\epsilon_t = 0.65$ since the experimentally observed range is typically between 0.6 and 0.7, and study variations for 300 kg $m^{-3} \leq \rho_b \leq$ 650 kg m^{-3}. The range of ρ_b values are obtained based on values reported for MOF and carbon samples in literature (Table 1). The gravimetric pellet loading, q_p for a given ρ_b value is illustrated in Fig. 2 at 3.5 MPa and 298 K. Using a similar procedure we evaluate the value of q_p at 1 bar and 30 $(V/V)_b$ based on a discharge capacity of 150 $(V/V)_b$ (Lozano-Castelló et al. 2002). Using the values at 30, 180 $(V/V)_b$ and the point of zero loading, we fit the Dubinin-Ashtakov (DA) equation (Dubinin and Astakhov 1971) to obtain the gravimetric pellet isotherm shown in Fig. 2.

2.2 Equilibrium isotherms

The Dubinin-Astakhov (DA) isotherm equation is,

$$q = \rho_{ads} W_0 \exp\left[-\left(\frac{A}{\beta E_0}\right)^n\right], \quad (6)$$

where, ρ_{ads} is the adsorbed gas density, W_0 is the microporous volume per unit mass of adsorbent, β is the affinity coefficient related to the adsorbate-adsorbent interaction, the value of which is 0.35 for methane adsorption (Stoeckli et al. 2000). We used a value of βE_0 = 8.4 kJ mol^{-1} with $W_0 = 1.67 \times 10^{-3}$ m^3 kg^{-1} and $n = 1.75$ for ρ_p = 461.5 kg m^{-3} and $W_0 = 0.76 \times 10^{-3}$ m^3 kg^{-1} and $n = 1.8$ at $\rho_p = 1,000$ kg m^{-3}. The values of A and ρ_{ads} are evaluated at the corresponding pressure and temperature. We point out that other model isotherms could also be used to depict the gravimetric loadings at intermediate pressures. Since our primary focus is the target loadings at 3.5 MPa and 298 K, our conclusions are independent of a precise choice for the isotherm. The values of the gravimetric capacity, q_p evaluated from Eq. 1 for ρ_b in the range of 300–650 kg m^{-3} are 0.38–0.175 kg/kg at 3.5 MPa and 298 K as illustrated in Fig. 2. The contribution from the gas phase (Eq. 1) to the mass of gas stored in the bed is 11.4 % at 3.5 MPa and 298 K. Changing ϵ_t to 0.7 results in a 12.3 % contribution from the gas phase.

2.3 Gravimetric capacity

The process of compacting the powder into pellets usually results in a loss in the gas adsorption capacity due to decreased accessible surface area and micropore volume, which lowers the adsorption capacity. However, compaction increases the material (pellet) density. Hence mapping the $(V/V)_p$ to $(V/V)_{pwd}$ is case specific and cannot be easily generalized. As a result it is more convenient, when discussing the powder targets, to work with the gravimetric adsorption capacities. Accounting for a 5–20 % loss in the gravimetric adsorption capacity (going from powder to pellet), the gravimetric loading at 3.5 MPa and 298 K for the powder samples range from 0.4 to 0.47 kg/kg at ρ_b = 300 kg m^{-3} and from 0.18 to 0.22 kg/kg at 650 kg m^{-3} to meet the storage target of 180 $(V/V)_b$ (Fig. 2 and Table 2). Using a similar procedure we evaluate the gravimetric adsorption capacities of powder and pellet samples at different storage targets ranging from 150 to 263 $(V/V)_b$ (see Table 2). At 263 $(V/V)_b$ which is the recently revised DOE target gravimetric loadings at the pellet range from 0.27 to 0.58 kg/kg setting a severe requirement on the gravimetric loading at the powder level. The corresponding $(V/V)_{pwd}$ for these materials would depend on their respective powder densities.

A recent compilation of MOF data indicate that the Zn_4O powder MOF samples show the highest gravimetric loading (0.13–0.17 kg/kg) (Mason et al. 2014) followed by the Cu_2 PCN family (0.16–0.19 kg/kg) (Makal et al. 2012; Mason et al. 2014). Whether these MOF materials meet the

Table 1 Packing density (ρ_b), pellet density (ρ_p), skeletal density (ρ_s), powder density (ρ_{pwd}) for activated carbon and MOF samples reported in the literature

Material	Method	ρ_b (kg m^{-3})	ρ_p (kg m^{-3})	ρ_s (kg m^{-3})	ρ_{pwd} (kg m^{-3})	Reference
MOF-5	0 % ENG[a]		310–790	2,030	130	Purewal et al. (2012)
	1 % ENG[a]		490			
	5 % ENG[a]		320–650			
	10 % ENG[a]		320–720			
MIL-53(AL)	Binder[b]	476				Finsy et al. (2009)
CPO-27-Ni	Mechanical compaction		780	2,600		Tagliabue et al. (2011)
HKUST-1	Mechanical compaction		640–824	2,800	430	Peng et al. (2013)
Ni/DOBDC	Mechanical compaction	400	780			Liu et al. (2012)
AC-CM	Mechanical compaction		560–990	1,900	240	Inomata et al. (2002)
C1050	Mechanical compaction		980		280	Guan et al. (2011)
PAC and ACP	Binder[c]		700,610		300–660	Jordá-Beneyto et al. (2008)
PAC and ACP	Binders[d]		400–1,000	1,900–2,160	510	Lozano-Castelló et al. (2002)
RP-20	Binder[b,e]	611			291	Balathanigaimani et al. (2008)
Ac, PFA-P, M-30, MSC-30	Hot pressing		340–890		210–300	Hou et al. (2007)
G216 carbon		410	631[f]	1,577[f]		Mota et al. (1997)
WV1050		280	686[f]	975[f]		Bastos-Neto et al. (2005)
MAXSORB III				2,200	300	Rahman et al. (2011); Loh et al. (2010)
IRH3		239[f]	341[f]	1,990		Momen et al. (2009)

AC-CM activated carbon prepared from cellulose microcrystals, *C1050* as-synthesized template carbon, *PAC* powdered activated carbon, *ACP* activated carbon pellets, *RP-20* monolith disks prepared from commercial activated carbon powder using PVA and PVP binders, *Ac* carbon powder prepared by acetylene, *CVD* chemical vapor deposition, *PFA-P* carbon powder prepared by carbonizing, *PFA* polyfurfuryl alcohol and deposited by propylene CVD over PFA-carbon/zeolite composite, *M-30 and MSC-30* commercial porous carbons activated with KOH, G216 carbon, WV1050, *IRH3* commercially obtained granular activated carbon, *MAXSORB III* commercially obtained activated carbon powder

[a] Expanded Natural Graphite

[b] *PVA* Polyvinyl alcohol

[c] *WSC* Polymeric binder from waterlink sutcliffe carbon

[d] *HAS* Humic acid derived sodium salt, PVA, binder from WSC, teflon, *ADH* adhesive cellulose-based binder

[e] *PVP* poly vinyl pyrrolidone

[f] Calculated from ϵ_t and ϵ_b values

targets would depend on the loss associated with pelletization. For MAXSORB III carbon based materials, gravimetric loadings for powdered samples of 0.23 kg/kg with ρ_b= 300 kg m^{-3} have been reported (Rahman et al. 2011; Loh et al. 2010). This corresponds to a loading of 124 $(V/V)_b$. From the data in Fig. 2 the minimum gravimetric pellet loading is uniquely specified once the bed density ρ_b and ϵ_t are fixed.

It is useful to determine the relation between q_p and the corresponding pellet density, ρ_p since the pellet density can be experimentally measured. Equation 4 can be used to obtain ρ_p by fixing the value of ϵ_b. The value of ϵ_b for adsorbent beds made up of pellets of activated carbons typically range from 0.3 to 0.35 (Mota et al. 1997; Sahoo et al. 2011). In what follows, we set $\epsilon_b = 0.35$ and use typical values for the material properties found in carbon based systems to illustrate the various losses encountered during gas storage. Since packed bed characteristics depend on the pellet shape and size, the bed porosities, ϵ_b for MOF pellets are expected to be similar. The measured values of packing density (ρ_b), pellet density (ρ_p), skeletal density (ρ_s), and powder density (ρ_{pwd}) reported in

Table 2 Gravimetric and volumetric capacity of pellet and powder samples for packed bed densities, ρ_b varying between 300 and 650 kg m^{-3} at different storage targets, $(V/V)_b$

Gravimetric capacity					
Storage target $(V/V)_b$	ρ_p kg m^{-3}	Powder kg/kg	Pellet kg/kg	Volumetric capacity $(V/V)_p$	% drop $\frac{(V/V)_p-(V/V)_b}{(V/V)_p}\times 100$
150	461.5	0.32–0.385	0.308	199	24.6
	615.4	0.243–0.29	0.231		
	1000	0.15–0.18	0.142		
180	461.5	0.4–0.47	0.38	245	26.5
	615.4	0.3–0.36	0.285		
	1000	0.22–0.185	0.175		
220	461.5	0.5–0.59	0.475	307	28
	615.4	0.376–0.45	0.357		
	1000	0.231–0.275	0.22		
263	461.5	0.61–0.72	0.578	373	29.5
	615.4	0.456–0.54	0.433		
	1000	0.28–0.33	0.267		

The corresponding pellet density (ρ_p) and volumetric capacity, $(V/V)_p$ of the pellet are calculated using Eqs. 4, 8 respectively. The ranges for the powder samples are obtained by assuming a 5–20 % loss due to pelletization

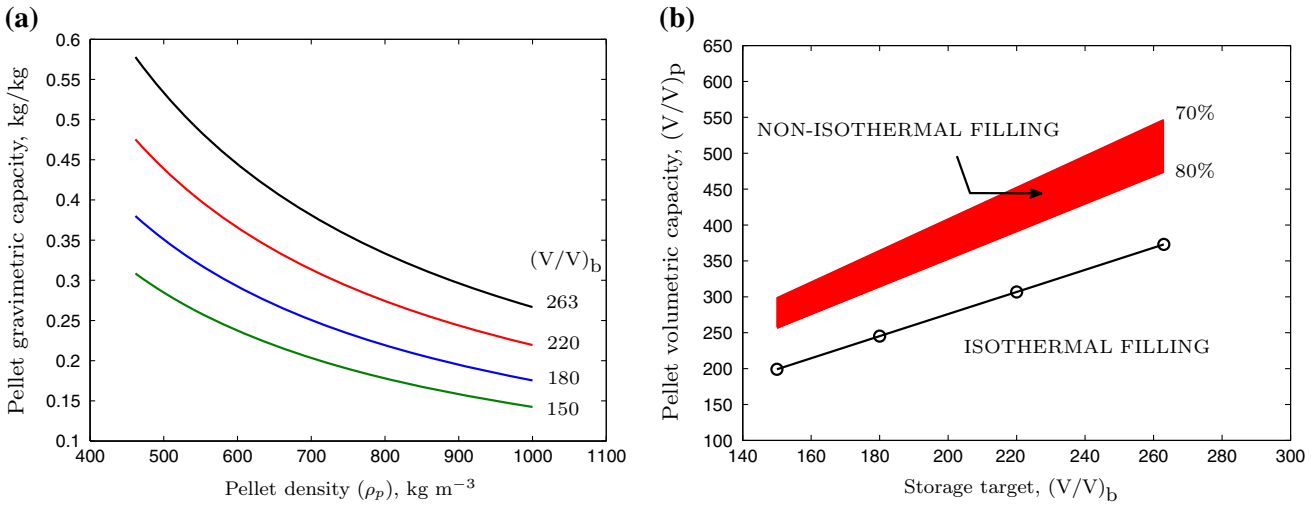

Fig. 3 **a** Variation of target pellet, gravimetric capacity with pellet density for different values of storage targets, $(V/V)_b$ at 298 K. **b** Pellet volumetric capacity with different storage targets, $(V/V)_b$ during isothermal and non-isothermal filling. The volumetric capacities of pellets are calculated based on storage targets achieved at the end of filling. The *red band* represents the variation in pellet volumetric capacity considering 70–80 % filling efficiencies due to non-isothermal effects. The *solid line* shows the pellet volumetric capacities for different storage targets under isothermal filling conditions. For data in (**a**), the packed bed density (ρ_b) is varied in the range of 300–650 kg m^{-3} with $\epsilon_b = 0.35$ and $\epsilon_t = 0.65$, b) $\epsilon_b = 0.35$ (Color figure online)

literature for MOF and carbon materials are shown in Table 1. Figure 3a illustrates the variation in the gravimetric capacity of the pelletized sample as a function of the pellet density ρ_p for 150, 180, 220 and 263 $(V/V)_b$ targets obtained using Eq. 1 with the corresponding mass of methane. For a fixed storage target an increase in the gravimetric capacity is observed as ρ_p decreases. The percentage change in the gravimetric loading between the capacities is the largest at the lowest pellet density. This data clearly illustrates the advantage of developing materials with a high pellet density to achieve storage targets. For a given pellet density, ρ_p, the gravimetric capacity q_p is finally determined by the microstructure of the material which influences properties such as the pore volume and surface area (Peng et al. 2013; Makal et al. 2012).

2.4 Volumetric storage capacity

Once the pellet isotherm has been determined, the adsorption isotherm for the packed bed is constructed using Eq. 1 by adding the gas contribution from the pore space or porosity in the adsorbent bed. The isotherm (on a V/V basis)

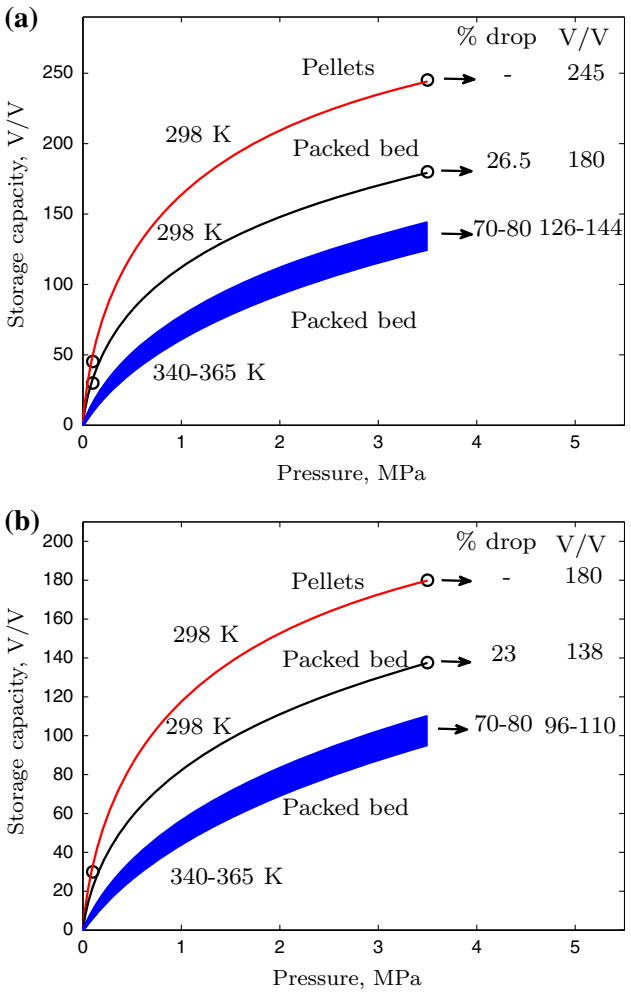

Fig. 4 Volumetric capacity (V/V) range for target materials. **a** A pellet capacity of 245 $(V/V)_p$ is required to meet the 180 $(V/V)_b$ target at 3.5 MPa and 298 K. Non-isothermal filling (340-365 K) results in a decrease to 126–144 $(V/V)_b$. **b** Capacity losses if the 180 (V/V) target was achieved for the pellet. The bed capacity drops to 138 $(V/V)_b$ at 3.5 MPa and a further drop to 96–110 $(V/V)_b$ occurs due to non-isothermal effects. *Red solid line* indicates storage capacity of pellet sample at 298 K, *black solid line* indicates storage capacity at packed bed at 298 K, *blue band* indicates storage capacity in packed bed stage during filling (Color figure online)

for the packed bed is illustrated in Fig. 4 by using the pellet isotherm (Fig. 2) corresponding to $\rho_b = 650$ kg m^{-3}. Note that all pellet isotherms regardless of the ρ_b values will yield the target loading of 180 $(V/V)_b$ since this was the basis for their construction in Fig. 2. In order to obtain the corresponding pellet isotherm the excess gas adsorbed in the pellet under STP conditions is evaluated from

$$(V/V)_p = \frac{22.414 \rho_p q_p}{M_g} \tag{7}$$

for q_p corresponding to $\rho_p = 1000$ kg m^{-3}. Substituting q_p from Eq. 1, and using Eq. 4, Eq. 7 reduces to,

$$(V/V)_p = \frac{22.414}{M_g}\left[\frac{1}{1-\epsilon_b}\left(\frac{m_g}{V_b} - \rho_g \epsilon_t\right)\right] \tag{8}$$

From Eq. 8 we observe that $(V/V)_p$ is only a function of the porosities, ϵ_t and ϵ_b which is related to the ratio of ρ_b/ρ_p (Eq. 4). The plot of $(V/V)_p$ is illustrated in Fig. 4a. At 35 bar and 298 K the corresponding value of $(V/V)_p$ is 245 in order to obtain a $(V/V)_b = 180$ at STP conditions. The $(V/V)_p$ for different $(V/V)_b$ targets is illustrated in Fig. 3b and Table 2. We show that in order to meet the $(V/V)_b$ storage targets varying from 150 to 263, the corresponding $(V/V)_p$ value calculated using Eq. 8 should lie between 199 and 373 for pellet densities ranging from 461.5 to 1000 kg m^{-3}.

In the above calculation we have not accounted for losses that accompany filling of the adsorbent bed under non-isothermal (exothermic) conditions. Due to the large temperature rise that accompanies adsorption in packed beds, filling efficiencies which depend strongly on the rate of filling typically vary between 70 and 80 %. This would further reduce the 180 $(V/V)_b$ capacity to 126–144 $(V/V)_b$ as illustrated in Fig. 4a for the DA isotherm. Accounting for this added loss, would set a more severe requirement on the capacity of the powder sample, since the $(V/V)_p$ would exceed 300 and 500 for storage targets of 180 and 263 $(V/V)_b$ respectively (Fig. 3b) for a larger drop of 70 % in filling efficiencies. High filling rates are desirable for onboard filling of the natural gas vehicle and this comes at a capacity loss at the filling station. This loss can be reduced significantly if filling is carried out off-board under near equilibrium (slow fill) conditions. We next illustrate the scenario starting from a pellet sample which meets the adsorption target of 180 $(V/V)_p$ at STP conditions (Fig. 4b). Using ρ_p in the same range as used earlier and assuming $\epsilon_b = 0.35$ the value of $(V/V)_b$ reduces to 138 as shown in Fig. 4b. A further drop in capacity to about 100 $(V/V)_b$ will occur if filling efficiencies are included.

3 Conclusions

Using typical values for carbon and MOF based adsorbents we illustrate the various losses in adsorption capacity that are encountered while taking a powder sample prepared in the laboratory to an onboard storage device. Effective compaction strategies in the powder to pellet transformation need to be devised to minimize gravimetric adsorption losses that typically lie in the range of 5–20 %. In packed beds, gas is primarily stored in the adsorbent pellet, however due to the inherent porosity of the bed gas is also stored in the compressed form making up about 11 % of the total mass of gas stored at 3.5 MPa. Solutions based on carbon monoliths circumvent both the above losses,

although one has to contend with the higher pressure drops associated with these adsorbent beds. Hence in order to meet the DOE 180 and revised 263 $(V/V)_b$ storage targets at the adsorbent bed level, the volumetric storage capacity of the pelletized sample should be at least 245 and 373 $(V/V)_p$ respectively if filling losses are ignored and above 300 and 500 $(V/V)_p$ if filling losses are taken into account. Hence evaluating a potential gas storage material based on the V/V at the powder level, as is the current practise, is only the first step to screen and select potential materials. Our analysis indicates, that determining the gravimetric capacity at the pellet level is more appropriate in order to fully assess the materials potential to meet the DOE storage targets at the level of the packed bed. Challenges lie in developing high specific surface area (Farha et al. 2012) materials, effective pelletization strategies and measuring pellet adsorption capacities (Peng et al. 2013) to realistically assess a materials potential for natural gas storage.

Acknowledgments This research was carried out under the Thematic Unit of Excellence on Computational Materials Science (TUECMS) Nanomission program, supported by the Department of Science and Technology (DST) India. BPP is grateful to TUECMS for financial support. BPP is also grateful to S. J Jaju for assisting with the graphics.

References

Balathanigaimani, M.S., Lee, M.J., Shim, W.G., Lee, J.W., Moon, H.: Charge and discharge of methane on phenol-based carbon monolith. Adsorption **14**(4–5), 525–532 (2008)

Bastos-Neto, M., Torres, A.E.B., Azevedo, D.C.S., Cavalcante Jr, C.L.: A theoretical and experimental study of charge and discharge cycles in a storage vessel for adsorbed natural gas. Adsorption **11**(2), 147–157 (2005)

Basumatary, R., Dutta, P., Prasad, M., Srinivasan, K.: Thermal modeling of activated carbon based adsorptive natural gas storage system. Carbon **43**(3), 541–549 (2005)

Biloé, S., Goetz, V., Guillot, A.: Optimal design of an activated carbon for an adsorbed natural gas storage system. Carbon **40**(8), 1295–1308 (2002)

Burchell, T., Rogers, M.: Low pressure storage of natural gas for vehicular applications. SAE Tech. Pap. Ser. **1**, 2000–2205 (2000)

Celzard, A., Albiniak, A., Jasienko-Halat, M., Marêché, J.F., Furdin, G.: Methane storage capacities and pore textures of active carbons undergoing mechanical densification. Carbon **43**(9), 1990–1999 (2005)

Dubinin, M.M., Astakhov, V.A.: Description of adsorption equilibrium of vapours on zeolites over wide ranges of temperature and pressure. Adv. Chem. Ser. **102**, 69 (1971)

Farha, O.K., Eryazici, I., Jeong, N.C., Hauser, B.G., Wilmer, C.E., Sarjeant, A.A., Snurr, R.Q., Nguyen, S.T., Yazaydın, A.O., Hupp, J.T.: Metal-organic framework materials with ultrahigh surface areas: Is the sky the limit? J. Am. Chem. Soc. **134**(36), 15,016–15,021 (2012)

Finsy, V., Ma, L., Alaerts, L., Vos, D.E.D., Baron, G.V., Denayer, J.F.M.: Separation of CO_2/CH_4 mixtures with the MIL-53(Al) metal-organic framework. Microporous Mesoporous Mater. **120**(3), 221–227 (2009)

Goetz, V., Biloé, S.: Efficient dynamic charge and discharge of an adsorbed natural gas storage system. Chem. Eng. Commun. **192**(7), 876–896 (2005)

Guan, C., Loo, L.S., Wang, K., Yang, C.: Methane storage in carbon pellets prepared via a binderless method. Energy Convers. Manage **52**(2), 1258–1262 (2011)

Hou, P.X., Orikasa, H., Itoi, H., Nishihara, H., Kyotani, T.: Densification of ordered microporous carbons and controlling their micropore size by hot-pressing. Carbon **45**(10), 2011–2016 (2007)

Inomata, K., Kanazawa, K., Urabe, Y., Hosono, H., Araki, T.: Natural gas storage in activated carbon pellets without a binder. Carbon **40**(1), 87–93 (2002)

Jordá-Beneyto, M., Lozano-Castelló, D., Suárez-García, F., Cazorla-Amorós, D., Linares-Solano, Á.: Advanced activated carbon monoliths and activated carbons for hydrogen storage. Microporous Mesoporous Mater. **112**(1), 235–242 (2008)

Konstas, K., Osl, T., Yang, Y., Batten, M., Burke, N., Hill, A.J., Hill, M.R.: Methane storage in metal organic frameworks. J. Mater. Chem. **22**(33), 16,698–16,708 (2012)

Kumar, V.S., Raghunathan, K., Kumar, S.: A lumped-parameter model for cryo-adsorber hydrogen storage tank. Int. J. Hydrogen Energy **34**(13), 5466–5475 (2009)

Liu, J., Tian, J., Thallapally, P.K., McGrail, B.P.: Selective CO_2 capture from flue gas using metal-organic frameworks-a fixed bed study. J. Phys. Chem. C **116**(17), 9575–9581 (2012)

Loh, W.S., Rahman, K.A., Chakraborty, A., Saha, B.B., Choo, Y.S., Khoo, B.C., Ng, K.C.: Improved isotherm data for adsorption of methane on activated carbons. J. Chem. Eng. Data **55**(8), 2840–2847 (2010)

Lozano-Castelló, D., Cazorla-Amorós, D., Linares-Solano, A., Quinn, D.F.: Activated carbon monoliths for methane storage: influence of binder. Carbon **40**(15), 2817–2825 (2002)

Lozano-Castelló, D., Alcañiz Monge, J., De la Casa-Lillo, M.A., Cazorla-Amorós, D., Linares-Solano, A.: Advances in the study of methane storage in porous carbonaceous materials. Fuel **81**(14), 1777–1803 (2002)

Makal, T.A., Li, J.R., Lu, W., Zhou, H.C.: Methane storage in advanced porous materials. Chem. Soc. Rev. **41**, 7761–7779 (2012)

Mason, J.A., Veenstra, M., Long, J.R.: Evaluating metal-organic frameworks for natural gas storage. Chem. Sci. **5**(1), 32–51 (2014)

Matranga, K.R., Myers, A.L., Glandt, E.D.: Storage of natural gas by adsorption on activated carbon. Chem. Eng. Sci. **47**(7), 1569–1579 (1992)

Momen, G., Hermosilla, G., Michau, A., Pons, M., Firdaous, M., Marty, P., Hassouni, K.: Experimental and numerical investigation of the thermal effects during hydrogen charging in packed bed storage tank. Int. J. Heat Mass Transfer. **52**(5), 1495–1503 (2009)

Mota, J.P.B., Rodrigues, A.E., Saatdjian, E., Tondeur, D.: Dynamics of natural gas adsorption storage systems employing activated carbon. Carbon **35**(9), 1259–1270 (1997)

Peng, Y., Krungleviciute, V., Eryazici, I., Hupp, J.T., Farha, O.K., Yildirim, T.: Methane storage in metal-organic frameworks: current records, surprise findings, and challenges. J. Am. Chem. Soc. **135**(32), 11,887–11,894 (2013)

Purewal, J., Liu, D., Sudik, A., Veenstra, M., Yang, J., Maurer, S., Müller, U., Siegel, D.J.: Improved hydrogen storage and thermal conductivity in high-density MOF-5 composites. J. Phys. Chem. C **116**(38), 20,199–20,212 (2012)

Rahman, K.A., Loh, W.S., Chakraborty, A., Saha, B.B., Chun, W.G., Ng, K.C.: Thermal enhancement of charge and discharge cycles for adsorbed natural gas storage. Appl. Therm. Eng. **31**(10), 1630–1639 (2011)

Sahoo, P.K., John, M., Newalkar, B.L., Choudhary, N.V., Ayappa, K.G.: Filling characteristics for an activated carbon based adsorbed natural gas storage system. Ind. Eng. Chem. Res. **50**(23), 13,000–13,011 (2011)

Sahoo, P.K., John, M., Newalkar, B.L., Choudhary, N.V., Ayappa, K.G.: Corrections to filling characteristics for an activated carbon based adsorbed natural gas storage system. Ind. Eng. Chem. Res. **53**(11), 4522–4523 (2014a)

Sahoo, P.K., Prajwal, B.P., Dasetty, S.K., John, M., Newalkar, B.L., Choudary, N.V., Ayappa, K.G.: Influence of exhaust gas heating and L/D ratios on the discharge efficiencies for an activated carbon natural gas storage system. Appl. Energy **119**, 190–203 (2014b)

Stoeckli, F., Guillot, A., Hugi-Cleary, D., Slasli, A.M.: Pore size distributions of active carbons assessed by different techniques. Carbon **38**, 938–941 (2000)

Sun, Y., Liu, C., Su, W., Zhou, Y., Zhou, L.: Principles of methane adsorption and natural gas storage. Adsorption **15**(2), 133–137 (2009)

Tagliabue, M., Rizzo, C., Millini, R., Dietzel, P.D.C., Blom, R., Zanardi, S.: Methane storage on CPO-27-Ni pellets. J. Porous Mater. **18**(3), 289–296 (2011)